



## Sorption isotherm and length change behavior of autoclaved aerated concrete



Lam Nguyen Trong<sup>a,c,\*</sup>, Shingo Asamoto<sup>a</sup>, Kunio Matsui<sup>b</sup>

<sup>a</sup> Department of Civil and Environmental Engineering, Saitama University, 255, Shimo-Okubo, Sakura-ku, Saitama, 338-8570, Japan

<sup>b</sup> Construction Materials Laboratory, Asahi Kasei Construction Materials Corporation, 106 Someya, Sakai, Ibaraki, 306-0493, Japan

<sup>c</sup> Department of Building Materials Technology, Faculty of Building Material, National University of Civil Engineering (NUCE), 55 Giai Phong Road, Hanoi, Viet Nam

### ARTICLE INFO

#### Keywords:

Autoclaved aerated concrete  
Pore size distribution  
Shrinkage recovery  
Shrinkage hysteresis  
Capillary tension  
Surface free energy

### ABSTRACT

We conducted an experimental study on the sorption isotherm and length change behavior of autoclaved aerated concrete (AAC) in both desorption and adsorption processes. Three types of AAC with different bulk densities were used to study the length change mechanism. The experimental results show that the expansion of AAC during the adsorption process is mostly larger than the shrinkage in the first desorption process even though the water content in the adsorption process is lower. Interestingly, a clear expansion in the desorption process in a range of relative humidity (RH) from about 90% to 65% and a significant difference in the length change strain between the desorption and adsorption processes (shrinkage hysteresis) at high RH are observed. Based on these experimental results, we propose a model to represent the mechanism of the hygral length change of AAC, taking into account the changes in surface free energy of the solid surface and capillary tension. The model reasonably explains the significantly different length change behaviors of AACs with different pore structures.

### 1. Introduction

Autoclaved aerated concrete (AAC) is a lightweight cementitious material. It is generally manufactured by autoclaving a mixture of finely ground silica materials (either in the form of silica sand or recycled materials), Portland cement, quicklime, water, gypsum, and an expanding agent (aluminum powder). AAC is cured under high temperature and saturated steam pressure (typically, reaching a pressure of 0.8–1.4 MPa and a temperature of 180–200 °C).

AAC has a unique structure, which is characterized by a solid skeleton and pores. The pore system of AAC consists of artificial air pores [1–7] and the pores in the skeletal material [1,3,6], which can be classified into inter-cluster pores and inter-particle pores [7], or macrocapillaries and microcapillaries [5]. The structure of AAC is also characterized by the types of reaction products, which mainly belong to the tobermorite group of calcium silicate hydrates [2,8–14].

Nowadays, AAC is widely used in many building applications due to advantages such as low density (resulting in dead load reduction and low haulage cost), low thermal conductivity, high heat resistance, fast building rate, and environmental friendliness. However, the length changes that accompany drying or wetting may cause the cracks in AAC as the result of external confinement. Such damage causes water leakage problems and accelerates the transport of corrosive agents that

cause corrosion of internal reinforcement steel.

The mechanism of hygroscopic volume change has been widely discussed in relation to other porous media, such as charcoal [15–19], activated carbon rods [20–22], and Vycor glass [23–25]. In these cases, the volume change is explained mainly by capillary tension and the change in surface free energy. This mechanism has also been considered for cementitious materials but it is not able to produce the pronounced hysteresis in the length change of hardened cement paste [26]. In the case of hardened cement paste, a linear relationship between length change at low relative humidity (RH) and change in surface free energy has been almost agreed [27,28]. Capillary pressure has also been identified as the principle shrinkage mechanism at high RH, as the presence of menisci has been established in that humidity range [27,29–32]. However, the influence of capillary tension has recently been called into question [25,33,34].

Several investigations of the drying shrinkage of AAC have been carried out [1,6,35,36], but the shrinkage was normally examined at a specific RH (35–45%). Ziembicka has interpreted the drying shrinkage of AAC with a capillary tension theory; he predicted that drying shrinkage is a function of volume and specific surface area of micro pores of radii 7.5–62.5 nm [36]. The capillary tension theory of drying shrinkage of porous building materials states that the water in the pore exists in tension and this creates an attractive force between the pore

\* Corresponding author. Department of Civil and Environmental Engineering, Saitama University, 255, Shimo-Okubo, Sakura-ku, Saitama, 338-8570, Japan.  
E-mail address: [lamnt@nuce.edu.vn](mailto:lamnt@nuce.edu.vn) (L. Nguyen Trong).

walls [23,37]. Georgiades suggested that drying shrinkage of AAC is a function of the specific surface area of fine pores of radii 2–20 nm [6]. However, the sorption isotherm and length change behavior of AAC have not yet been fully examined for the whole range of conditions from saturated to dry at various RHs and consequently the length change mechanism of AAC is still not clear.

In this study, we experimentally investigated the sorption isotherm and length change behavior of AAC at various RHs in both desorption and adsorption processes. The mechanisms of volumetric change in porous cementitious systems are intimately related to their microstructure, including pore size distribution, surface area, and morphology of hydrate solids [38–40]. Therefore, the aim of this paper is to relate the hygral length change of AACs to their pore structure, especially the pore size distribution. Based on the experimental results, a model is proposed to explain the length change behavior of AAC materials. Since the chemical composition of AAC is similar to that of cement paste, an understanding of the length change mechanism in AAC could also be expected to clarify the shrinkage mechanism of hardened cement paste, which has been discussed for a long time.

## 2. Materials and methods

### 2.1. Materials

The AAC materials were selected for experiment to investigate the length change behavior and relate the hygral length change to its pore structure. In this study, three types of AAC produced by different manufacturers in Japan and Vietnam, which were expected to have different pore characteristics, were used for the experiments. The AAC that was manufactured in Japan is denoted by JP and the two types that were manufactured in Vietnam are denoted by VN1 and VN2.

The chemical composition of AACs, which was analyzed by X-ray fluorescence, is shown in Table 1. The crystal phase of AACs is mainly quartz and tobermorite according to x-ray diffraction, as shown in Fig. 1. These AAC materials have a similar composition, but differ in basic physical properties, such as bulk density, total porosity, and pore-size distribution. The pore size distributions of the AAC materials, which were determined by mercury intrusion porosimetry (MIP), are shown in Fig. 2. The pore-size distribution curves of VN2 is single peak, whereas the JP and VN1 are bimodal. However, the volume of fine pores, for which the pore radius is around 10 nm, is much higher in JP (about 0.594 ml/g) than in VN1 (about 0.372 ml/g). The bimodal pore size distribution of AAC has been reported by Mitsuda [41], Kreft [42], and Jerman [43], while the pore size distribution of AAC with the single peak was reported by Chen [44]. Some other basic physical properties are summarized in Table 2.

**Table 1**  
Chemical composition of AACs.

Oxide, %	VN1	VN2	JP
SiO <sub>2</sub>	50.33	51.69	58.94
Al <sub>2</sub> O <sub>3</sub>	3.43	3.15	1.72
Fe <sub>2</sub> O <sub>3</sub>	1.69	1.66	0.88
CaO	27.68	28.31	26.56
MgO	1.04	1.19	0.46
SO <sub>3</sub>	1.89	1.78	1.25
Na <sub>2</sub> O	0.17	0.13	0.14
K <sub>2</sub> O	1.04	1.00	0.16
TiO <sub>2</sub>	0.21	0.19	0.12
P <sub>2</sub> O <sub>5</sub>	0.03	0.03	0.05
MnO	0.02	0.03	0.03
Cr <sub>2</sub> O <sub>3</sub>	0.05	0.03	0.01
SrO	0.02	0.03	0.02
L.O.I	12.39	10.77	9.67

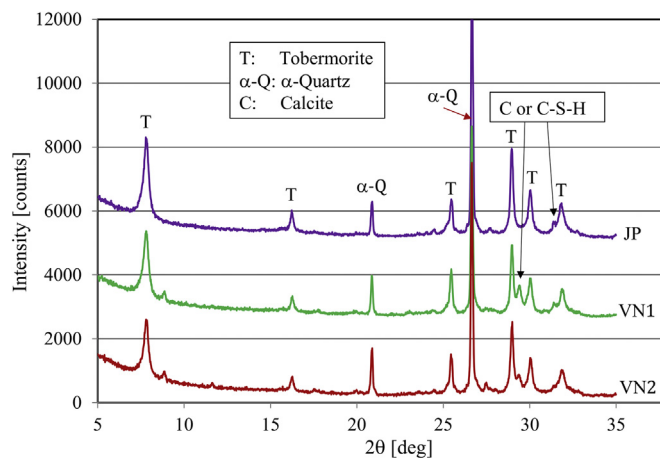


**Fig. 1.** X-ray diffraction patterns of the AAC materials.

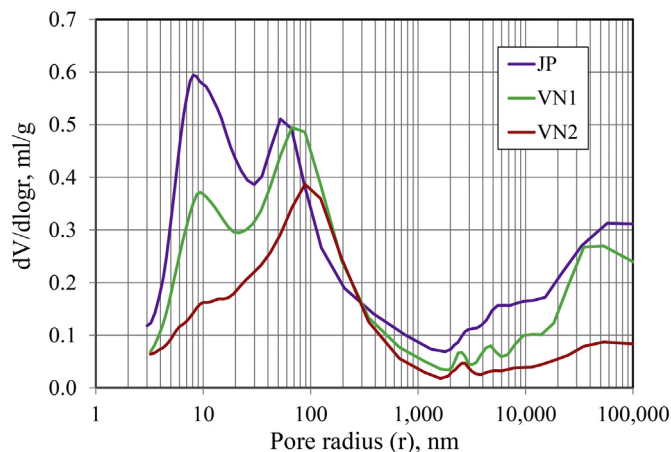


**Fig. 2.** Pore size distributions of the AAC materials.

**Table 2**  
Physical properties of the AACs.

Materials	Bulk density [kg·m <sup>-3</sup> ]	Matrix density [kg·m <sup>-3</sup> ]	Total porosity [% vol]
JP	510	2130	76.1
VN1	420	2525	83.4
VN2	650	2455	73.5

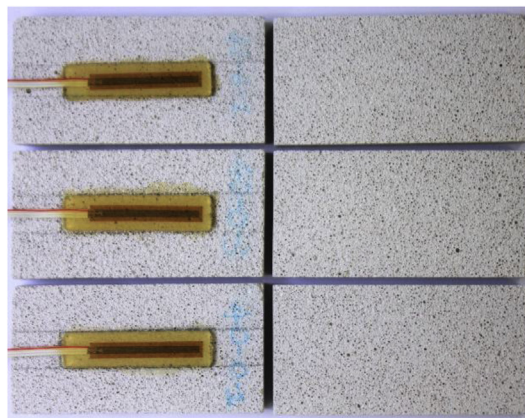


**Fig. 3.** AAC specimens.

Download English Version:

<https://daneshyari.com/en/article/10128339>

Download Persian Version:

<https://daneshyari.com/article/10128339>

[Daneshyari.com](https://daneshyari.com)